Science
AAAS

Supplementary Materials for

Recovery of particulate methane monooxygenase structure and activity in a lipid bilayer

Christopher W. Koo, Frank J. Tucci, Yuan He, Amy C. Rosenzweig*

Correspondence to: amyr@northwestern.edu

This PDF file includes:

Materials and Methods

Methanotroph growth

Methanotrophs were cultured in 12 L of media using a BioFlo 4500 fermentor (New Brunswick Scientific) following established protocols (*8, 10, 43*). *M. capsulatus* (Bath) was cultured in 1 X nitrate mineral salts media, 3.9 mM phosphate buffer, pH 6.8, supplemented with 80 µM NaFeEDTA, 50 µM $CuSO_4 \cdot 5H_2O$, and trace element solution at 45 °C and a continuous flow of 1 L/min at a 1:3 ratio of methane:air. Cells were harvested at an OD_{600} of 8-10, pelleted, and flash frozen in liquid nitrogen. *Methyocystis* sp. str. Rockwell was cultured in salt solution, 3.9 mM phosphate buffer, pH 6.8, supplemented with 40 µM $FeSO_4$, 50 µM $CuSO_4 \cdot 5H_2O$, and trace elements solution at 30 °C and a continuous flow of a 1:4 ratio of methane:air. *M. alcaliphilum* comb. nov. 20Z was grown in 1 X nitrate mineral salts media, 0.5 M NaCl, 2.3 mM phosphate buffer, pH 6.8, 50 mM carbonate buffer, pH 9.5, 40 µM $CuSO_4 \cdot 5H_2O$, and trace element solution at 30 °C and a continuous flow of a 1:3 ratio of methane:air.

Isolation of pMMO

Membranes were isolated according to previous methods (*11*). *M. capsulatus* (Bath) and *M. alcaliphilum* comb. nov. 20Z cell pellets were thawed in 25 mM PIPES, pH 7.3, 250 mM NaCl. For *Methylocystis* sp. str. Rockwell cell pellets, $CuSO_4 \cdot 5H_2O$ was added to a concentration of 500 µM (*10*). Cells were lysed by sonication on ice at 35% amplitude with 1 s alternating pulses for 9 min (Qsonica Q700). Lysed cells were subjected to two rounds of centrifugation at 10,000 x g for 45 and 25 min, discarding the pellet after each cycle. The supernatant was then centrifuged at 150,000 x g for 1 h to pellet the membranes. The supernatant was discarded, and the membrane fraction was subjected to 2 rounds of homogenization using a Dounce homogenizer in 25 mM PIPES, pH 7.3, 250 mM NaCl followed by centrifugation to re-pellet the membranes at 150,000 x g for 30 min. Following the last round of centrifugation, the membranes were homogenized in 7 ml of the same buffer, aliquoted, flash frozen, and stored at -80°C. The concentration of protein in the membranes was measured using the DC Lowry assay (Bio-Rad) with BSA as a standard.

pMMO was solubilized from the membranes using n-dodecyl-β-D-maltopyranoside (DDM). Membranes were thawed on ice, and DDM was added at a ratio of 1.2 mg DDM:1 mg pMMO, followed by mixing end-over-end at 15 rpm for 1 h at 4 °C. To remove remaining membranes and aggregated protein, the mixture was centrifuged for 1 h at 150,000 x g, and the pellet was discarded. Solubilized pMMO was then exchanged into buffer containing 25 mM PIPES pH 7.3, 250 mM NaCl, and 0.02% DDM using Amicon concentrators (MilliporeSigma) with a molecular weight cutoff of 100 kDa. The concentration was measured using the DC Lowry (Bio-Rad) assay with BSA as a standard, pMMO was diluted to a concentration of 10 mg/ml, and aliquots were flash frozen and stored at -80 °C.

Membrane scaffold protein expression and purification

Plasmid pMSP1E3D1 (Addgene) was transformed into *E. coli* BL21 Star (DE3) cells and grown on LB-agar plates containing 30 µg/ml kanamycin. Cultures were grown in 5 ml LB for 18 h and then in 200 ml LB for 18 h. The 200 ml culture was used to inoculate 12 L TB media at an optical density at 600 nm (OD_{600}) of ~0.1 and shaken at 180 rpm at 37 °C. Expression of MSP1E3D1 was induced at an OD_{600} of ~2.4 (~4 h) by adding 1 mM IPTG. Cells were then grown for 4 h at 37 °C, harvested by centrifugation at 8000 x g for 15 min, flash frozen, and stored at -80 °C. Each 12 L TB culture yielded ~60 g of cells.

Cell pellets were thawed in Tris buffer containing 40 mM Tris, pH 7.3, 250 mM NaCl, and 10 mM imidazole with 1% Triton X-100, DNase (Sigma), and Protease Inhibitor Cocktail (Roche). Cells were lysed by sonication on ice with 1 s pulse on 2 s pulse off for 10 min (Qsonica Q700). The lysate was centrifuged for 30 min at 10,000 x g to remove insoluble aggregates. The soluble fraction was then applied to a gravity column containing 10 ml NiNTA beads. The column was washed with 5 column volumes (cv) Tris buffer with 50 mM sodium cholate, followed by 15 cv Tris buffer. The protein was eluted with 5 cv Tris buffer containing 250 mM imidazole. TEV protease was added to the eluted protein at a ratio of 1:20 protease:protein and dialyzed overnight at 4 °C against Tris buffer containing 1 mM EDTA. TEV protease and uncleaved protein were then removed by flowing over the NiNTA column and collecting the flow-through. MSPs were concentrated and buffer-exchanged into 25 mM PIPES, pH 7.3, 250 mM NaCl in an Amicon concentrator (MilliporeSigma) with a 10 kDa molecular weight cutoff to ~4 mg/ml, measured by nanodrop A_{280} using a molecular weight of 30,110 kDa and an extinction coefficient of 26,930 M^{-1} cm^{-1}. Aliquots were flash frozen and stored at -80 °C.

Lipid preparation

DMPC and POPC solubilized in chloroform (Avanti) were dried down to a thin layer in a glass vial at room temperature under a stream of nitrogen gas and then stored overnight in a vacuum desiccator to remove remaining trace amounts of chloroform. These dried lipids (25 mg per vial) were resolubilized in 25 mM PIPES, pH 7.3, 250 mM NaCl, and100 mM sodium cholate to a final lipid concentration of 50 mM.

For native lipids, *M. capsulatus* (Bath) cell pellets were thawed and resuspended in 20 ml methanol per 1 g cells. The suspension was homogenized in a Dounce homogenizer with an additional 10 ml dichloromethane and 5 ml 40 mM phosphate buffer, pH 7.4. The organic and aqueous layers were allowed to separate overnight, and the organic layer was then removed by aspiration. The organic layer was dried under a stream of nitrogen to form an oily layer, which was dried further in a vacuum desiccator overnight.

The weight of dried lipids was measured, and an approximately 50 mM stock solution of solubilized lipids was prepared by assuming an average molecular mass of 700 g/mol for extracted native lipids. The lipids were solubilized in 25 mM PIPES, pH 7.3, 250 mM NaCl, and 100 mM sodium cholate. To fully resuspend, the solubilized lipids were alternately heated at 50 °C, vortexed, and soaked in an ultrasonic bath for 20 s each until the lipids were fully dissolved. This stock was then aliquoted and frozen at -20 °C for later use. Typically, one gram of cells yielded ~20-40 mg of dry lipids from *M. capsulatus* (Bath).

Lipidomics

Lipidomics analysis was performed by Cayman Chemical (Ann Arbor, MI). Internal standards, including TG (16:0-d9/16:0/16:0), SM (d18:1/16:0-d9), DG (16:0-d9/16:0), CE (16:0-d9), PC (16:0-d9/16:0), PE (16:0-d9/16:0), PI (16:0-d9/16:0), PS (16:0-d9/16:0), and LysoPC (16:0-d9/0:0) were added to *M. capsulatus* (Bath) whole cells and native lipid nanodiscs along with 1 ml phosphate buffered saline:methanol 1:1 (v/v). This mixture was homogenized using a Precellys homogenizer using three 30 s cycles at 8000 rpm, with a 3 min rest interval on ice between cycles.

A methyl-tert-butyl ether (MTBE)-based liquid-liquid extraction procedure was then used. After adding 4 mL MTBE to each sample and vortexing vigorously, the mixture was incubated on a tabletop shaker at 500 rpm at room temperature for 1 h. Phase separation was

induced by the addition of 1 ml water. The samples were shaken for 10 min, and then centrifuged at 2000 x g for 15 min. The upper organic phase of each sample was carefully removed using a Pasteur pipette and transferred into a fresh glass tube. The remaining aqueous phase was reextracted with 2.5 mL of MTBE:methanol:water 10:3:2.5 (v/v/v). After vortexing and centrifuging as above, the organic phase was collected and combined with the initial organic phase. The extracted lipids were dried in a SpeedVac vacuum concentrator. The dried lipid extracts were reconstituted in 200 µl n-butanol:methanol 1:1 (v/v) and transferred into autosampler vials for lipidomic analysis by LC-MS/MS.

Lipostar (Version1.3.1b18; Molecular Discovery) software was used for feature detection, noise and artifact reduction, alignment, normalization, and lipid identification. Peak picking, smoothing, and retention time alignment were performed to identify unique *m/z* and retention time features. A retention time window filter of 1-32 min was used. Background peaks that appeared in blank solvent were removed along with peaks that did not contain MS/MS spectra, peaks that did not present any isotope pattern, and background noise.

Automated lipid identification was performed using the Lipid Maps database. This database includes major lipid classes (phospholipids, sphingolipids, DAGs, TAGs, and sterols) for both positive- and negative-ion modes and has been modified by Cayman to include extra lipids (e.g. many additional cardiolipins and some internal standards). The identification algorithm uses the detected accurate-mass m/z with a 5-ppm mass tolerance filter, as well as the corresponding MS/MS spectrum to identify lipids and ranks the identifications via a 1-to-4-star scale of increasing confidence. One-star ranked identifications were excluded. The integrated areas of all identified lipids were normalized to the integrated area of their corresponding class-specific internal standard. Identifications of the five most abundant molecular species in each class (sorted by their peak area ratio) were manually reviewed using MS/MS spectra and peak integration.

Nanodisc reconstitution

pMMO was reconstituted into nanodiscs following established protocols (*18, 44*). The following procedures were all conducted at 4 °C. pMMO in 0.02% DDM was mixed with lipids, MSP, and $CuSO_4$ at specific ratios and mixed end-over-end at 15 rpm for 30 min. For DMPC, a molar ratio of 1:75:240 pMMO:lipid:MSP was used. For POPC and native lipids, a molar ratio of 1:60:240 was used. Since pMMO is isolated from the native organism and has no affinity tag, a ratio of MSP:pMMO was chosen at one pMMO particle per disc to minimize the amount of empty nanodiscs present. SM-2 Bio-Beads (Bio-Rad) were added at 0.8 mg/ml and mixed end-over-end at 15 rpm for 2 h. Washed Bio-Beads were prepared by soaking in buffer containing 25 mM PIPES, pH 7.3 and 250 mM NaCl and decanting the mixture over a dry weigh boat. The weight of wet Bio-Beads was measured by removing liquid using a Pasteur pipette until no more could be removed. Bio-Beads were removed from the nanodisc mixture by passing through a 0.22 µm syringe filter. The formed nanodiscs were then concentrated using an Amicon concentrator (MilliporeSigma) with a molecular weight cutoff of 100 kDa and purified by size exclusion chromatography on a Superose 6 Increase 10/300 GL column (Cytiva) in buffer containing 25 mM PIPES pH 7.3 and 250 mM sodium chloride. Peak fractions were collected and concentrated. The concentration was measured using established methods to isolate empty nanodiscs from nanodiscs containing pMMO (*14*). Solubilized pMMO of known concentration was loaded onto a 15% SDS-PAGE gel at concentrations 4, 2, and 1 mg/mL alongside a sample of nanodisc-embedded pMMO. ImageJ was used to generate a standard curve, correlating the

band intensity of the PmoB subunit to protein concentration. The concentration of the nanodisc-embedded pMMO sample was then determined by comparing the intensity of the PmoB band to the standard curve.

Activity assay

The methane oxidation activity assay was conducted according to established methods (*11, 23*). For each assay, 100 µl pMMO, diluted to 1-5 mg ml^{-1}, either membrane-bound, DDM-solubilized or embedded in nanodiscs, was mixed with reductant (excess duroquinol) in 2-ml screw-top vials with septa tops (Agilent). 1 ml of air was removed from the vial and 1.5 ml of [^{13}C]methane was added. The mixture was shaken at 200 rpm in a water bath (45 °C for *M. capsulatus* (Bath) or 30 °C for *Methylocystis* sp. str. Rockwell and *M. alcaliphilum* comb. nov. 20Z) for 5 min followed by incubation on ice for 10 min. Negative controls were performed in the absence of [^{13}C]methane, duroquinol, or pMMO.

Samples were then prepared for GC/MS analysis. Chloroform (500 µl) containing 1 mM dicholoromethane was added to each sample. The samples were mixed at 2000 rpm for 10 min at 4 °C and centrifuged at 2000 x g for 10 min. 2.5 µl of sample was applied to a PoraBOND Q column (25 m x 250 µm x 3 µm) on an Agilent 7890B/5977A MSD GC/MS instrument with a split ratio of 10:1. The GC was maintained under a constant helium gas flow of 1.2 ml min^{-1}. The initial oven temperature was maintained at 80 °C for 3.5 min, increased at 50 °C min^{-1} to 150 °C, and held for 1.5 min. A second ramp rate of 15 °C min^{-1} was maintained until a final temperature of 300 °C was reached and held for 1 min. The mass spectrometer was maintained at a temperature of 230 °C, quad temperature of 150 °C, 70 eV, and a detector voltage of 2,999 V. Masses 31, 33, and 49 were monitored for the detection of ^{12}C-methanol, ^{13}C-methanol, and dichloromethane. The ^{13}C-methanol peak was integrated, quantified from a standard curve, and normalized to the concentration of dichloromethane.

ICP-MS

Samples were prepared by mixing 5-50 µl of analyte with 180 µl of 100% nitric acid and heating at 60 °C for 4 h. The sample was then diluted to 6 ml with metal-free water. The samples were analyzed using an iCAP Q ICP-MS instrument (Thermo) in the Quantitative Bioelemental Imaging Facility (QBIC) at Northwestern University.

Bioinformatics

The PmoC sequence logo was generated from 318 representative sequences from PF04896 and TIGR03078, manually selected from 451 sequences for those located in a pMMO or AMO operon, excluding "rogue" *pmoC* and *amoC* sequences. These representative sequences were clustered at 100% identity against a hidden Markov model constructed from 132 representative nodes clustered at 50% identity using the EFI-EST webtool. Sequences were aligned using MAFFT (*45*) in L-INS-I mode and gaps were removed using the *M. capsulatus* (Bath) PmoC sequence as a reference. The logo visualization was generated in Jalview (*46*).

Negative stain sample preparation and data processing

Negative stain samples were prepared at ~0.01 mg/ml protein concentration for nanodisc-embedded pMMO. 3 µl samples were applied to 400-mesh carbon-coated copper grids (Electron Microscopy Sciences) plasma cleaned at 30 W for 10 s with a Solarus plasma cleaner (Gatan). Grids were allowed to incubate in open air at room temperature for 1 min before blotting with

filter paper. Grids were then washed in two successive 50 µl drops of water for 15 s each followed by two successive 50 µl drops of 0.75% uranyl formate for 15 s each with manual agitation. Grids were blotted with filter paper and allowed to dry before storage in a grid box.

Images of the grids were collected using a JEM-1400 transmission electron microscope (JEOL) at 30,000x magnification and a pixel size of 3.71 Å. Images were collected using Leginon (*47*) at defocus values of 3-6 µm, and 2D class averages were determined using Appion (*48*).

CryoEM sample preparation

Samples were prepared by plunge freezing in liquid ethane using a Vitrobot Mark IV (Thermo Fisher). 3 µl of 1 mg/ml sample was applied to either 300- or 400-mesh C-flat holey carbon copper grids with 1.2 µm diameter and 1.3 µm spacing. Both 300- and 400-mesh grids yielded similar results, except that 300-mesh grids occasionally had more broken squares. Grids were prepared by plasma cleaning with a Solarus plasma cleaner (Gatan) for 10 s at a voltage of 10 W. The sample was incubated on the grid for 30 s in 100% humidity at 4 °C before dual-sided blotting for 4 s with a blot force of 7 and plunging into liquid ethane and storage under liquid nitrogen.

CryoEM data collection

CryoEM screening was performed using a JEM-3200FS transmission electron microscope (JEOL) with a K2 Summit Direct Detector (Gatan) at 300 kV. Data were collected at a magnification of 30,000x and a pixel size of 1.06 Å. Movie series with defocus values of 1.5-4.5 µm were collected using Leginon (*47*). Forty-frame exposures were taken at 0.3 s per frame using a dose rate of 8 e^{-} A^{-2} per movie series. Full cryoEM datasets were collected at three national facilities (Stanford-SLAC Cryo-EM Center (S^2C^2), National Center for CryoEM Access and Training (NCCAT), Pacific Northwest Center for CryoEM (PNCC)) using a Titan Krios (Thermo-Fisher) electron microscope at 300 kV with calibrated magnifications of 40,000 x and 30,000 x and pixel sizes of 0.86 Å and 1.06 Å. Movie series with varying numbers of frames, dosages, and defocus values were collected as detailed in Table S2.

CryoEM data processing

Frames were aligned using Relion's (version 3.1.0) (*49, 50*) implementation of Motioncorr to correct for specimen motion. CTF parameters were estimated using CTFFIND4 (*51*). Relion autopicking using Laplacian of Gaussian parameters was used to automatically select particles from micrographs (figs. S5, S6, and S20). All subsequent three-dimensional classification and refinement steps were performed with Relion (version 3.1.0). Particles were extracted with a box size of 256 pixels or 200 pixels, binned by 4. For dataset MC01, an initial round of 2D classification was performed. For all datasets except MC02 and MC03, two rounds of 3D classification were performed. All 3D class averaging was performed using C1 symmetry and maps generated from the corresponding crystal structure as a reference, low pass filtered to 20 Å. For each dataset, the initial masked reconstruction was obtained followed by refinement of CTF parameters. C3 symmetry was used throughout at this point. Following another round of 3D reconstruction, particles were polished using Relion's implementation. Following another masked 3D reconstruction, CTF parameters were refined again resulting in a gain in resolution of ~0.5-1 Å from first to last reconstruction in the process. Masks of varying tightness were generated, and the map was postprocessed with these masks to achieve the highest resolution

without cutting into the map. The final resolutions and B-factors of each map are included in Table S1.

Further processing techniques were then tested. Symmetry expansion followed by signal subtraction and 3D classification with and without alignment were performed to investigate potential differences between each protomer in the pMMO trimer, but no differences were observed. The nanodisc was masked out and the pMMO particle was subtracted, but again did not improve resolution or result in any differences between the maps. The maps were also processed with C1 symmetry, resulting in no differences in the maps except a slightly lower resolution.

Structure building

Models were built using Coot (*52*) and Phenix (*53*) software. The crystal structures were used as starting models (*M. capsulatus* (Bath) pMMO, PDB 3RGB; *M. alcaliphilum* comb. nov. 20Z pMMO, PDB 6CXH; *Methylocystis* sp. str. Rockwell pMMO, PDB 4PHZ), and new residues and ligands were built manually in Coot. The models were refined using the real space refine tool in Phenix. Residues were then manually inspected in Coot, and adjusted using the refine range tool. The douse program in the Phenix cryoEM suite (*53*) was used to identify water molecules in maps MC01-04, 20Z01, and RW01. The maps were inspected at multiple B-factor values in each region using the sharpen/blur tool on maps produced from the postprocess step in Relion at a manually inputted B-factor of zero. In some cases, the maps were also resampled at a higher rate using Coot in order to generate smooth densities, especially for waters and metal ions. ChimeraX was used to fit structures into density and to generate figures (*54, 55*).

Potassium cyanide treatment

Membranes from *M. capsulatus* (Bath) were treated with 50 mM potassium cyanide (KCN) according to established methods (*10, 42*). The membranes were first resuspended in 50 mM MOPS, pH 8.0, 250 mM NaCl, and 50 mM ascorbate using a Dounce homogenizer. Solid KCN was added to 50 mM, and the sample was incubated for 30 min at 4 °C with stirring in a fume hood, noting when the color changed from brown to pale. Membranes were recovered by ultracentrifugation at 150,000 x g for 45 min, taking care to add and remove tubes to and from the rotor in a fume hood. Membranes were washed by resuspending in MOPS buffer using a Dounce homogenizer and centrifuged again at 150,000 x g for 45 min. This procedure was repeated twice for a total of three washes before a final resuspension in MOPS buffer. The concentration was measured using the DC Lowry assay (Bio-Rad), and metal removal was confirmed by ICP-MS (fig. S19). Aliquots were stored at 4 °C for up to two weeks.

To reconstitute KCN-treated pMMO into nanodiscs, pMMO was solubilized from KCN-treated membranes with DDM as described above. For KCN-treated, copper reloaded samples,10 equivalents $CuSO_4$ (based on crude membrane protein concentration) was incubated with the membranes for 2 h at 4 °C prior to solubilization of pMMO. Nanodisc reconstitution was performed as above, and ICP-MS was used to measure the amount of $CuSO_4$ retained in the final nanodisc samples (fig. S19).

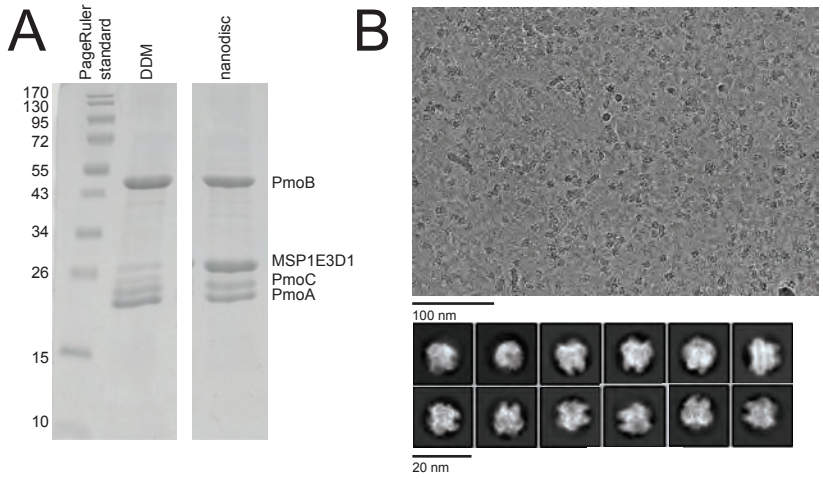

Fig. S1. Reconstitution of pMMO into lipid nanodiscs. (**A**) SDS-PAGE gel with bands corresponding to subunits PmoA, PmoB, PmoC, and the membrane scaffold protein MSP1E3D1. The lane labeled DDM contains DDM-solubilized pMMO before mixing with MSP1E3D1. Lanes are from the same gel with intermediate lanes removed for simplicity. (**B**) CryoEM micrograph showing pMMO nanodiscs and the corresponding 2D class averages.

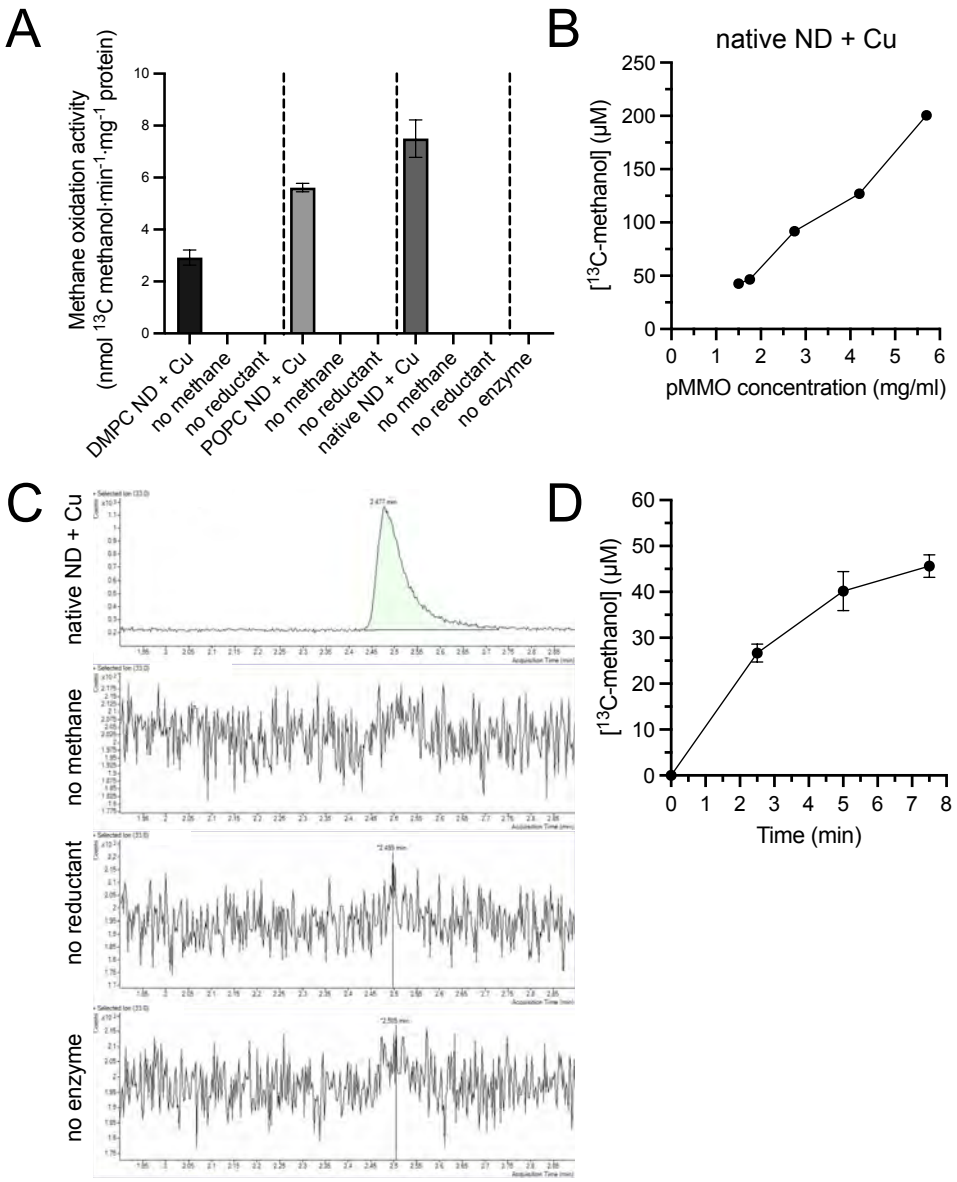

Fig. S2. Methane oxidation activity assay data. (**A**) Methane oxidation activity of pMMO reconstituted into nanodiscs (ND) in the presence of 3 equivalents of $CuSO_4$ (+ Cu) with varying lipids and the corresponding control reactions. Error bars represent standard deviation of $n \geq 3$ biological replicates, each measured in triplicate. (**B**) ^{13}C-methanol produced in the activity assay at varying concentrations of pMMO. Each datapoint represents 3 measurements (error bar too small to show). (**C**) GC/MS traces detecting the +33 ion corresponding to ^{13}C-methanol for the native ND + Cu sample. The area under peaks was integrated to determine ion count and the ^{13}C-methanol concentration. (**D**) Time-dependent production of ^{13}C-methanol for 1 mg/ml pMMO reconstituted into native ND with 3 equivalents of $CuSO_4$ added during reconstitution. Error bars represent standard deviation of $n \geq 3$ biological replicates, each measured in triplicate.

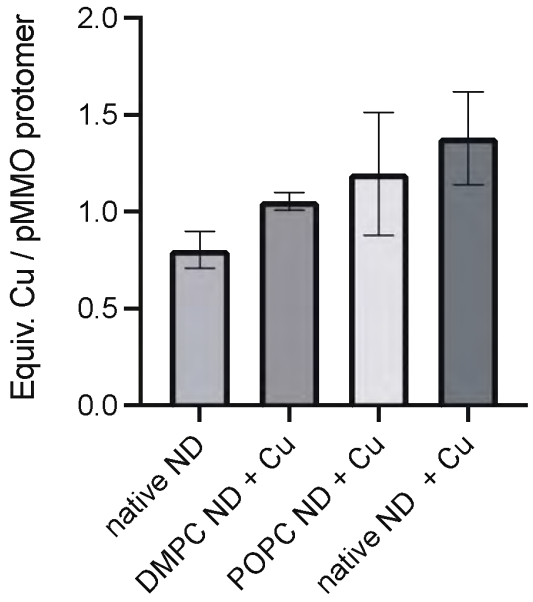

Fig. S3. Copper content of *M. capsulatus* (Bath) nanodiscs with synthetic and native lipids. Three equivalents of $CuSO_4$ were added to the "+ Cu" samples. Error bars represent standard deviation of $n \geq 3$ biological replicates, each measured in triplicate.

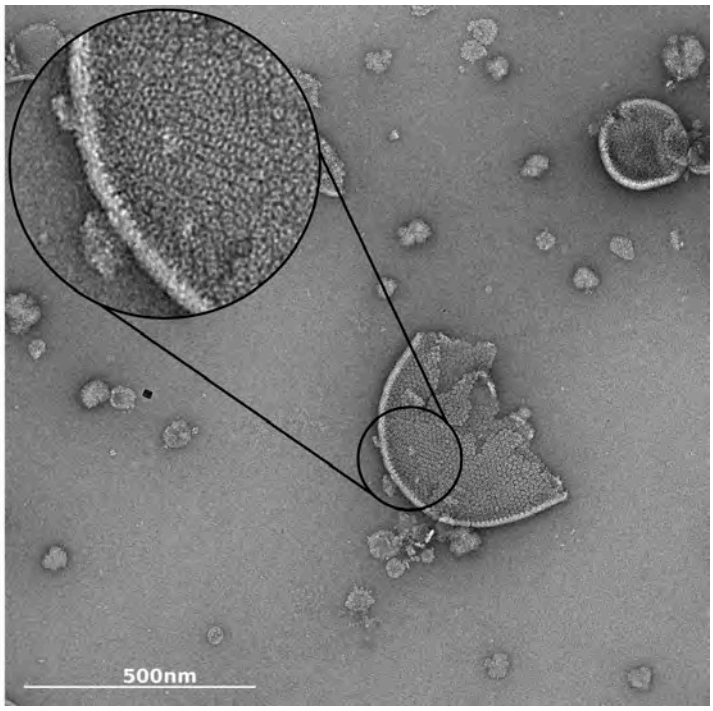

Fig. S4. Negative stain EM micrograph of *M. capsulatus* (Bath) isolated membranes. Tightly packed pMMO trimers are clearly visible in the membrane.

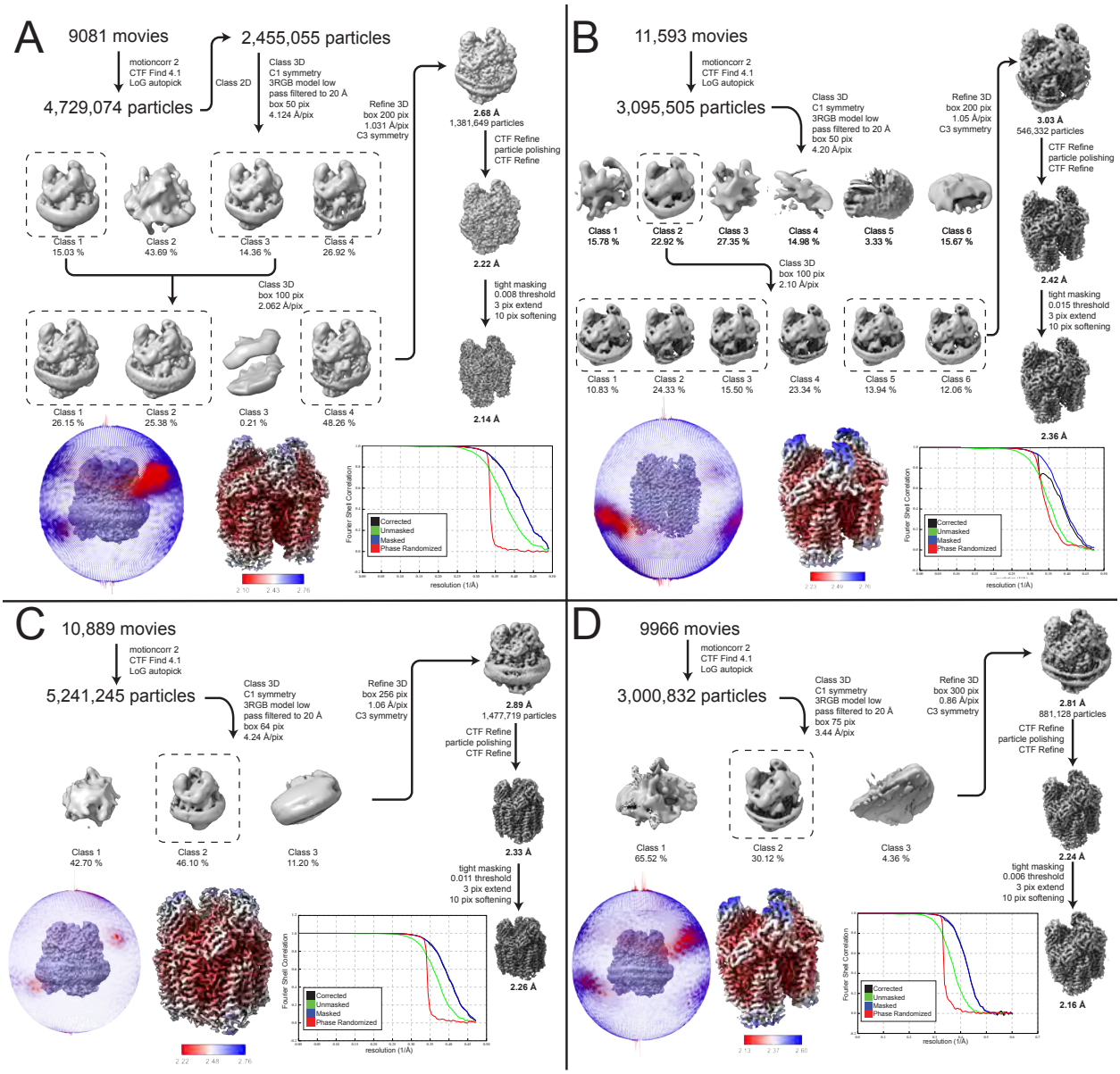

Fig. S5. Processing pipeline for *M. capsulatus* (Bath) cryoEM maps using Relion v3.1.0, including the Euler angle distribution, local resolution determined by Relion's implementation, and FSC curve for each final masked reconstruction. (**A**) MC01 dataset. (**B**) MC04 dataset. (**C**) MC02 dataset. (**D**) MC03 dataset.

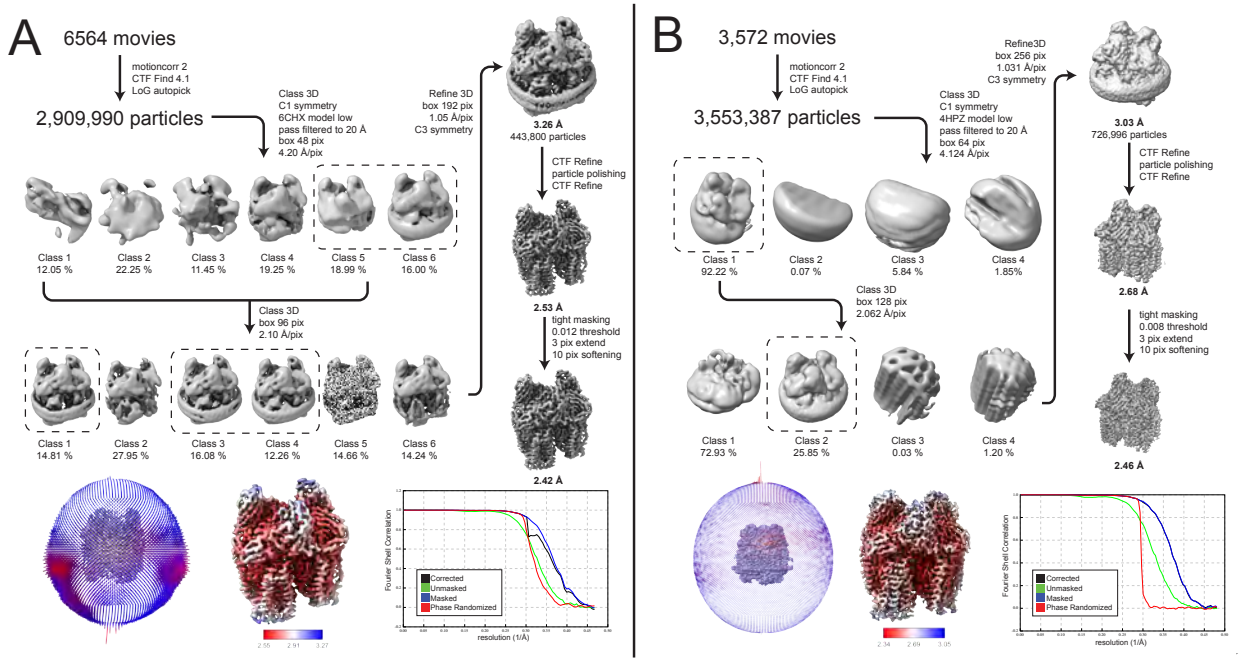

Fig. S6. Processing pipeline for *M. alcaliphilum* comb. nov. 20Z and *Methylocystis* sp. str. Rockwell using Relion v3.1.0, including the Euler angle distribution, local resolution determined by Relion's implementation, and FSC curve for each final masked reconstruction. (**A**) 20Z01 dataset. (**B**) RW01 dataset.

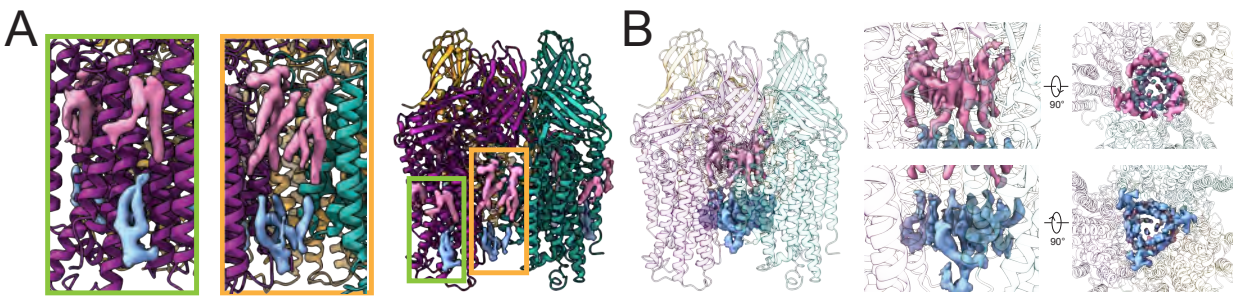

Fig. S7. Lipid densities in *M. capsulatus* (Bath) cryoEM map (MC01). The three symmetric protomers are shown in purple, teal, and gold. Lipids in the periplasmic leaflet of the bilayer are shown in pink, and cytoplasmic leaflet lipids are shown in blue. (**A**) Lipids on the periphery of pMMO. (**B**) Lipids on the interior pore of pMMO with side-on views of each leaflet and views from top-down and bottom-up showing the packing of lipids within the bilayer.

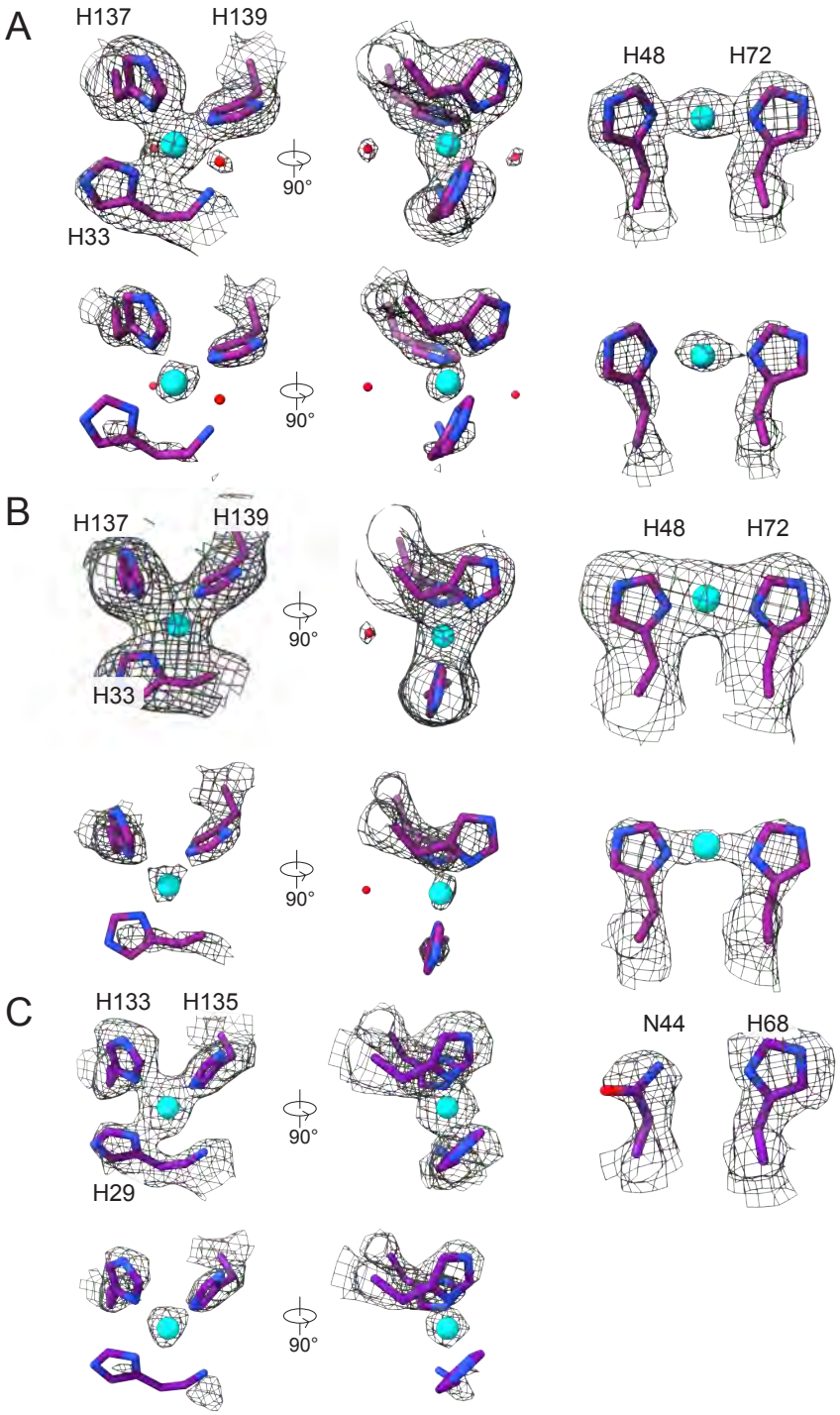

Fig S8. Cu_B site and bis-His site in cryoEM maps. (**A**) pMMO from *M. capsulatus* (Bath) resolved to 2.14 Å (MC01) is shown at two thresholds (0.026 and 0.056). At the higher threshold, it is clear that each site is mononuclear. (**B**) pMMO from *M. alcaliphilum* comb. nov. 20Z resolved to 2.44 Å (20Z01). (**C**) pMMO from *Methylocystis* sp. str. Rockwell resolved to 2.42 Å (RW01). The bis-His site is not conserved in this species and residue Asn44 corresponds to the missing histidine.

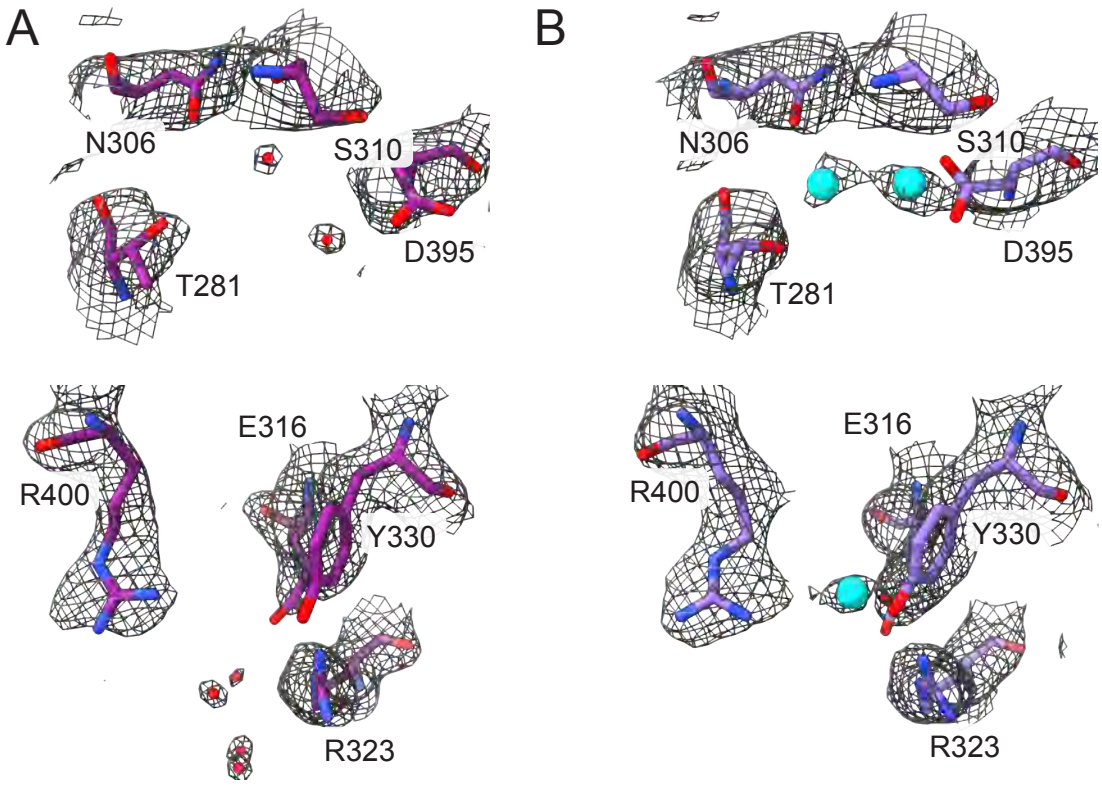

Fig. S9. CryoEM density at the proposed "copper sponge" site in the PmoB subunit of *M. capsulatus* (Bath) pMMO. (**A**) The 2.14 Å resolution map (MC01, this study) and model of active pMMO in native lipid nanodiscs shown at 0.018 threshold. (**B**) The 2.6 Å resolution model (PDB 7EV9) and map (EMDB 31325) of pMMO in detergent shown at 0.6 threshold. At this threshold level, where water molecules are visible in (**A**), there is no evidence for copper ions at this site.

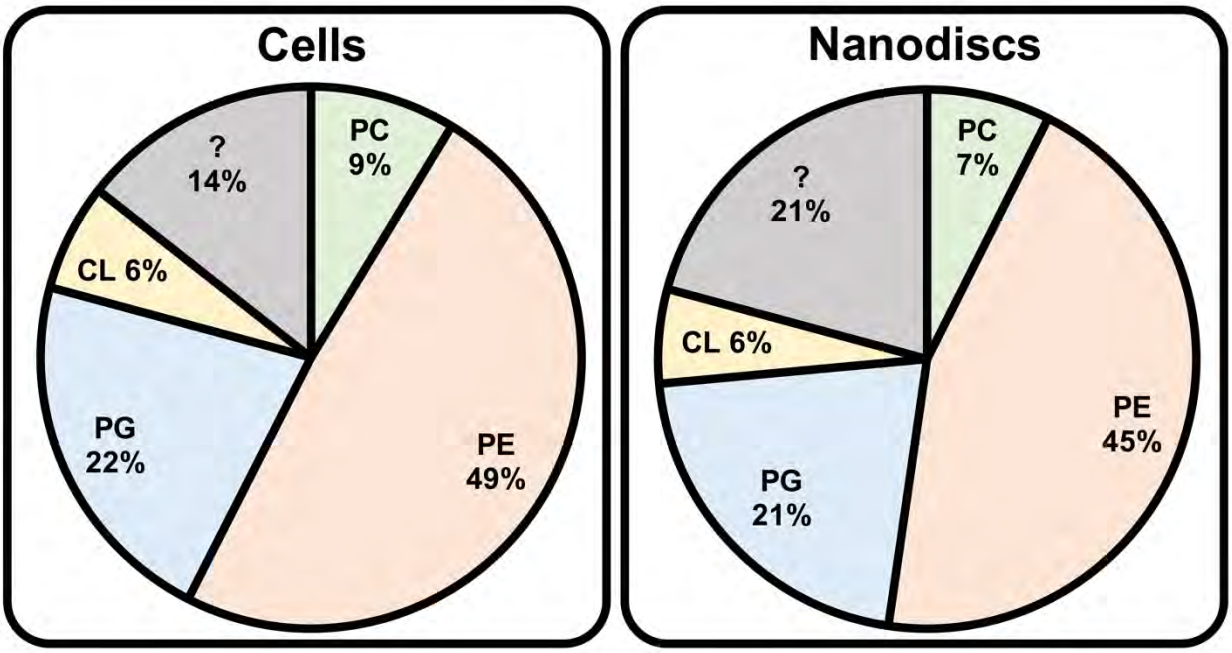

Fig. S10. Distribution of different classes of lipids in *M. capsulatus* (Bath) whole cells and *M. capsulatus* (Bath) pMMO reconstituted into native lipid nanodiscs.
Phosphatidylethanolamine (PE), phosphatidylcholine (PC), phosphatidylglycerol (PG), and cardiolipin (CL) were identified. A percentage of the lipids in each sample could not be identified (gray).

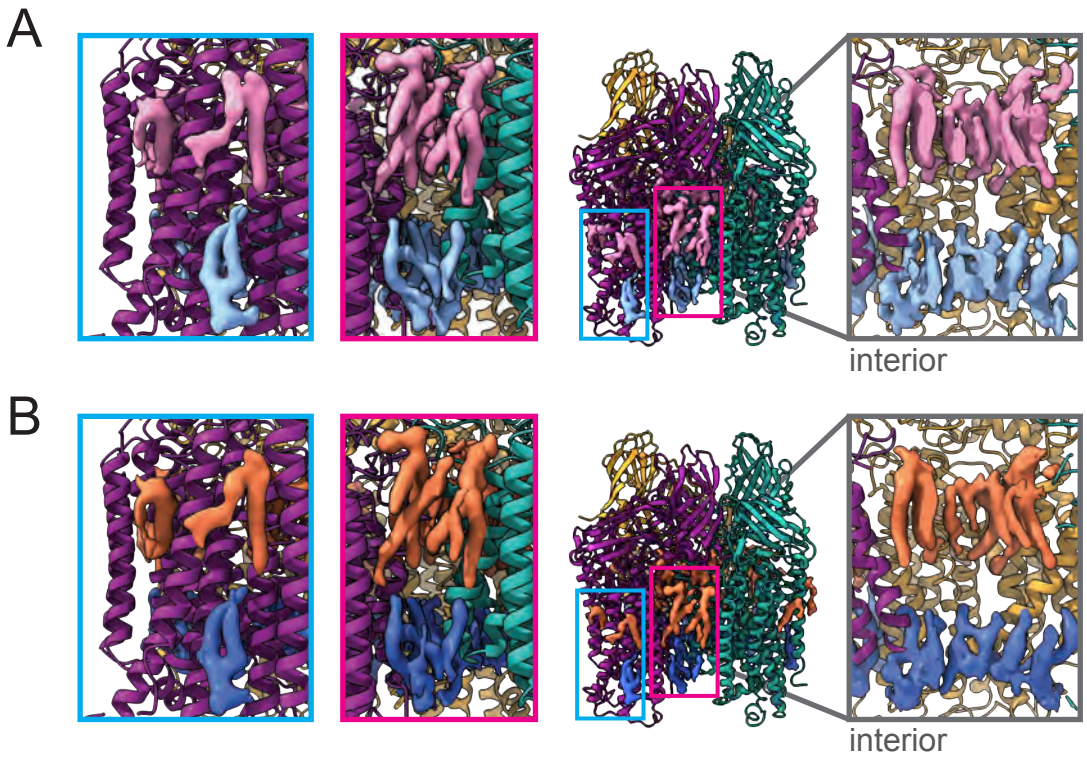

Fig. S11. Comparison of lipid densities between structures of pMMO in native lipid (MC01) and POPC (MC02) nanodiscs. (**A**) Model and densities from map MC01. Native periplasmic lipids are in pink and cytoplasmic lipids are in light blue. (**B**) Model and densities from map MC02. POPC periplasmic lipids are in orange and cytoplasmic lipids are in dark blue. The left panels show lipids on the exterior of the enzyme while the right panels show lipids on the interior of the pore. Yellow arrows (left panels) denote lipid densities whose headgroups are significantly different from other well-defined lipids.

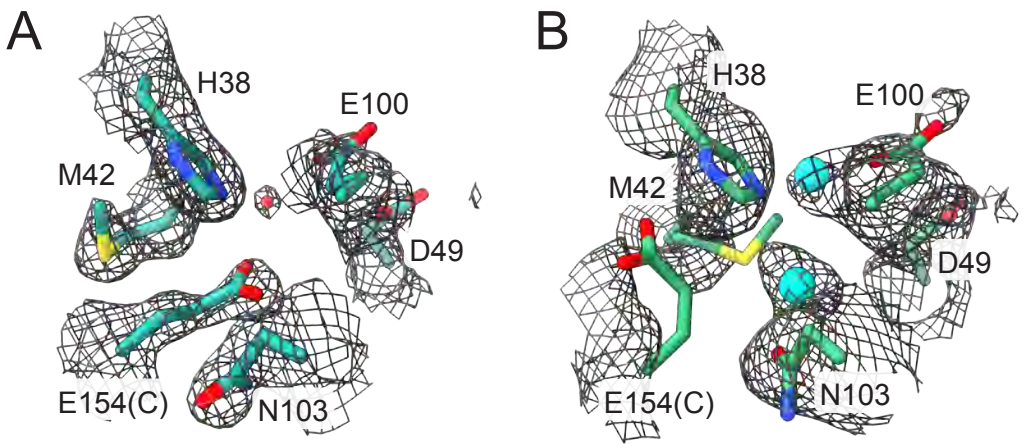

Fig. S12. CryoEM density at the proposed "trinuclear" copper site in the PmoA subunit of *M. capsulatus* (Bath) pMMO. (**A**) The 2.14 Å resolution map (MC01, this study) and model of the active pMMO in native lipid nanodiscs shown at 0.034 threshold. (**B**) The 2.6 Å resolution model (PDB 7EV9) and map (EMDB 31325) of pMMO in detergent shown at 0.42 threshold. At this threshold level where waters are visible, there is no evidence for a trinuclear copper center. Instead, residue E154 from PmoC fits into the density assigned as copper in 7EV9. A water is modeled in MC01 in the density assigned as a second copper ion in 7EV9.

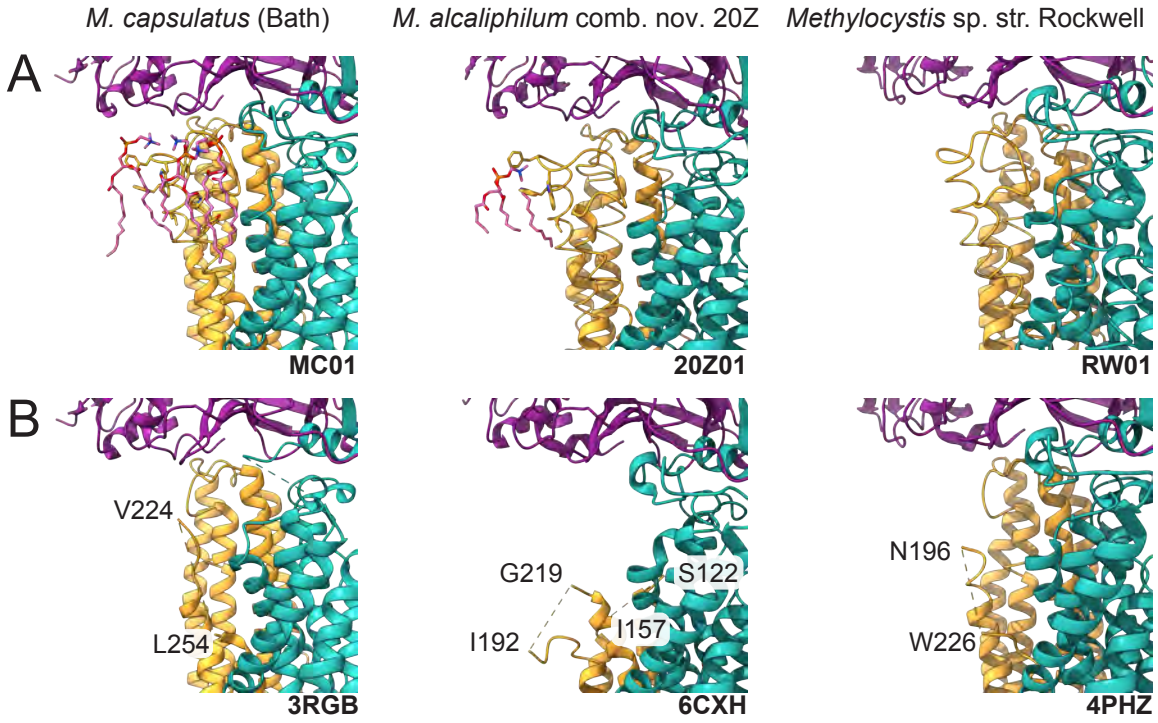

Fig. S13. Conserved region of PmoC newly observed in the cryoEM maps. (**A**) Models based on the cryoEM maps. (**B**) Crystal structures of pMMO from each species. PmoB is colored in purple, PmoA in teal, and PmoC in gold. The terminal residues adjacent to the missing regions are labeled.

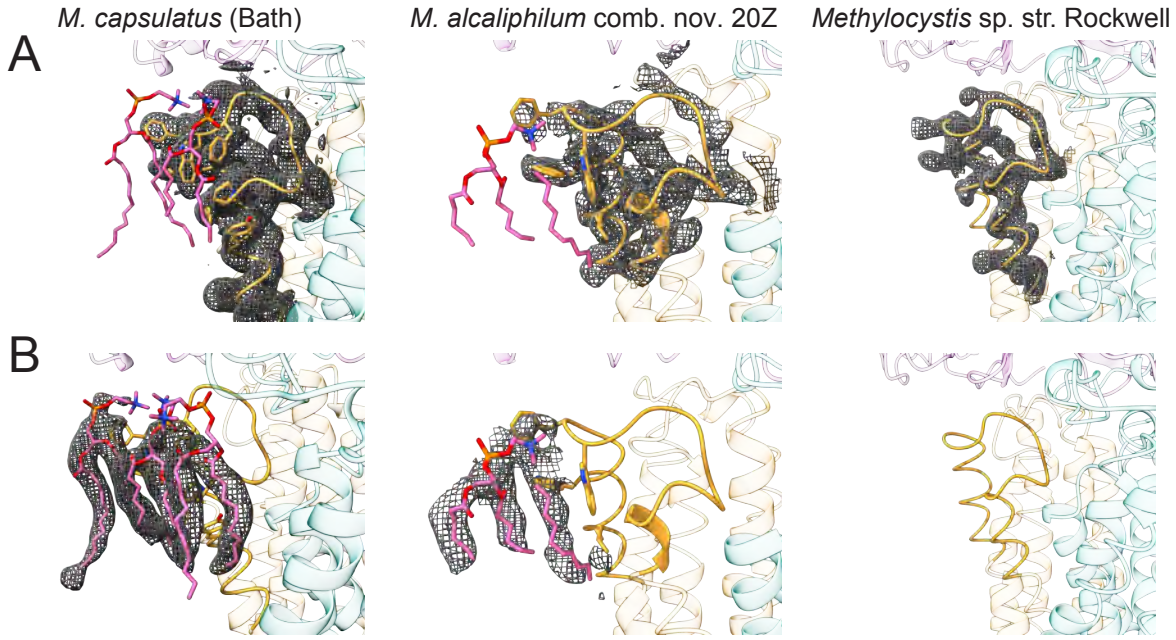

Fig. S14. Densities for conserved region of PmoC and neighboring lipids. (**A**) CryoEM map corresponding to the region missing in the crystal structures. (**B**) Models of the new region with density for stabilizing inner lipids. Residues that interact with lipids (< 4 Å distance) include *M. capsulatus* (Bath) PmoC residues Leu226, Trp229, Phe233, Trp234, Phe235, Pro243, and Tyr246 and *M. alcaliphilum* comb. nov. 20Z PmoC residues Leu198, Trp201, Phe205, and Phe206. While there is density present at the corresponding positions in the map of *Methylocystis* sp. str. Rockwell pMMO (RW01), lipids could not be fit definitively into this density.

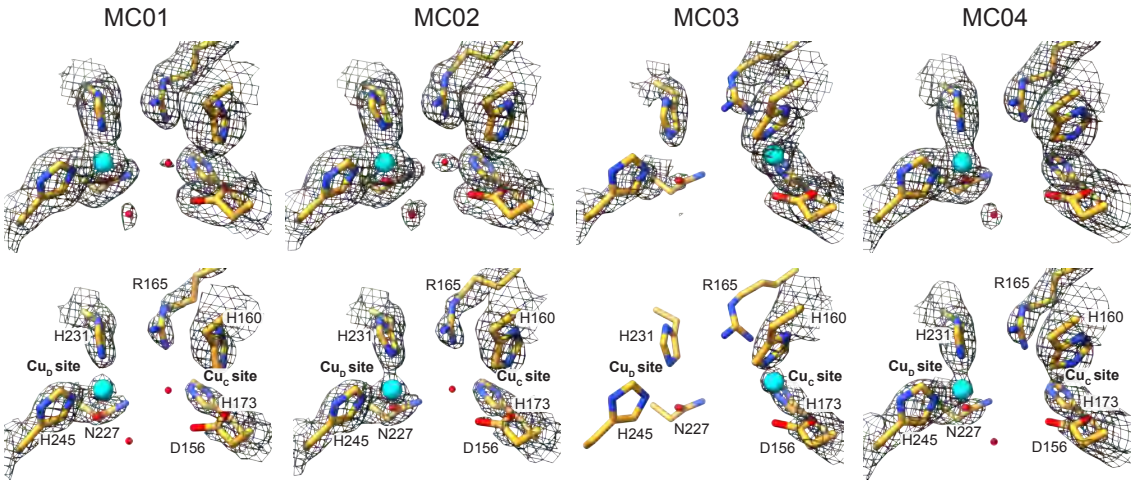

Fig. S15. CryoEM density for copper ions at Cu_C and Cu_D in native lipid (MC01, MC03, MC04) and POPC (MC02) nanodiscs. Each map is shown at two thresholds, showing mononuclear density for Cu_D in MC01, MC02 and MC04 and mononuclear density for Cu_C in MC03 at the higher threshold.

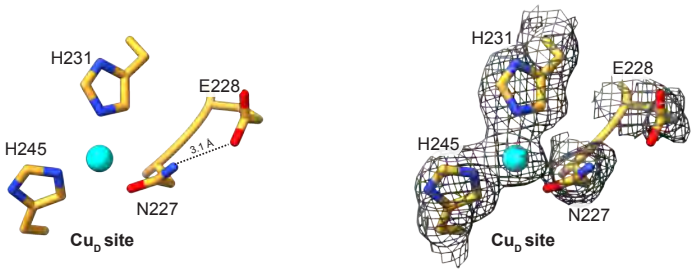

Fig. S16. Coordination of Asn227 to Cu$_D$ site. A hydrogen bond between Glu228 and Asn227 positions the side chain oxygen of Asn227 to coordinate copper.

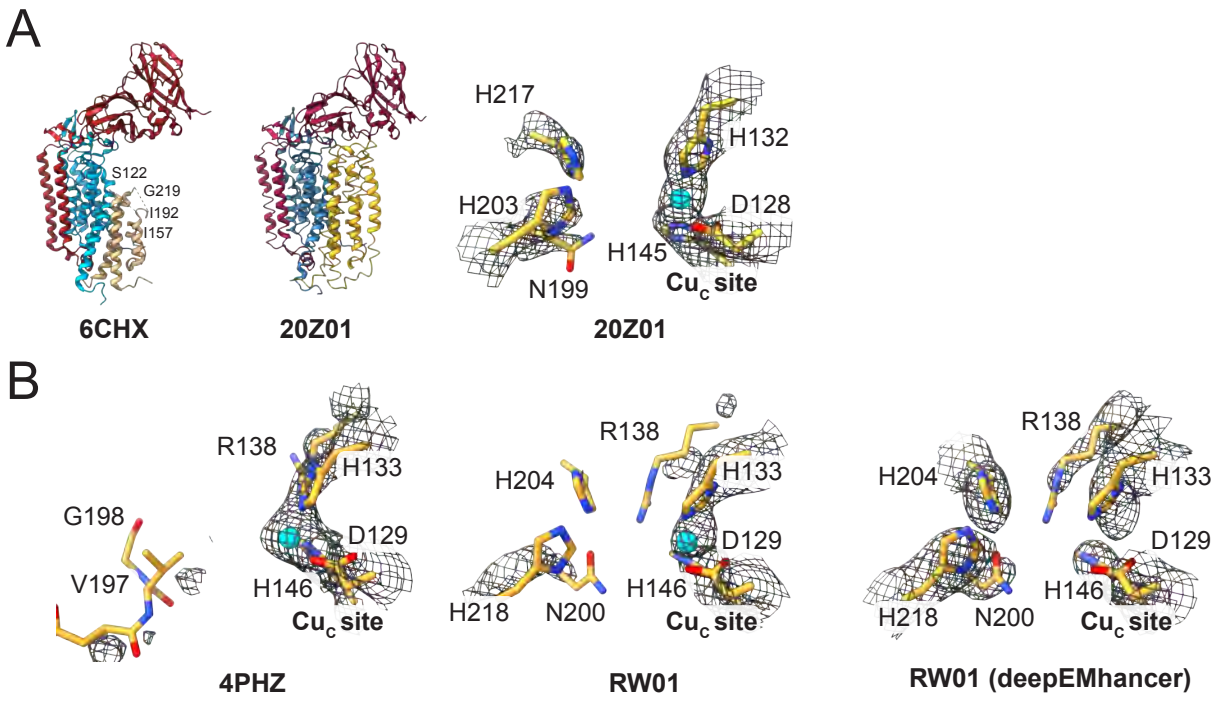

Fig. S17. Copper binding sites in *M. alcaliphilum* comb. nov. 20Z and *Methylocystis* sp. str. Rockwell PmoC subunits. (**A**) Comparison of the *M. alcaliphilum* comb. nov. 20Z crystal structure and cryoEM structure. The Cu_C site and surrounding region is completely missing in the crystal structure, whereas residues 20-89, 123-156, and 193-218 are visible in the cryoEM density. The Cu_C site is occupied in the nanodisc structure, although the residue corresponding to Arg165 in *M. capsulatus* (Bath) PmoC (Arg137) is missing. (**B**) Comparison of the *Methylocystis* sp. str. Rockwell crystal structure and cryoEM structure. DeepEMhancer (*37*) was used to fit the Cu_D residues Asn200, His204, His218, and Arg138.

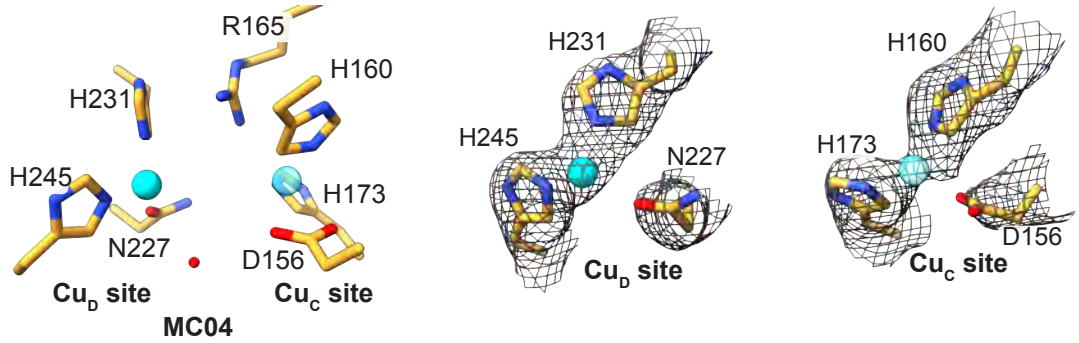

Fig S18 Alternate views of MC04 model and density showing density possibly corresponding to a copper ion at the Cu$_C$ site. The water molecule present in Cu$_C$ in MC01 and MC02 is missing while the density is continuous, suggesting that there may be copper in this site at low occupancy.

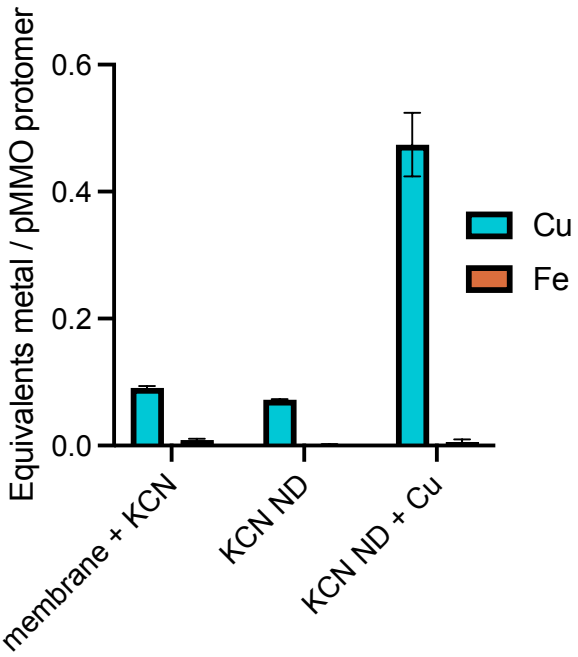

Fig S19. ICP-MS analysis of pMMO treated with potassium cyanide (KCN). Membrane + KCN, isolated *M. capsulatus* (Bath) membranes treated with KCN; KCN ND, nanodiscs formed with pMMO from the KCN-treated membranes and native lipids; KCN ND + Cu, copper added back to KCN-treated membranes followed by pMMO isolation from those membranes and reconstitution into nanodiscs with native lipids. Error bars represent standard deviation of n = 3 biological replicates, each measured in triplicate.

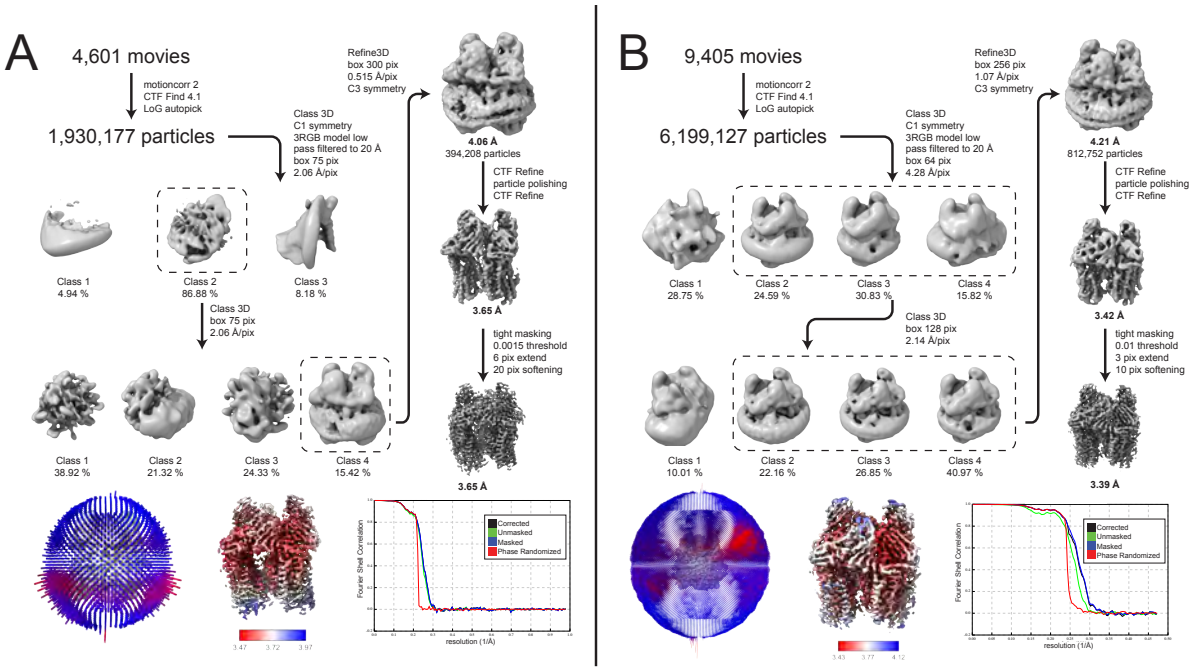

Fig. S20. Processing pipeline for *M. capsulatus* (Bath) samples treated with potassium cyanide, including the local resolution determined by Relion's implementation and FSC curve for each final masked reconstruction. (**A**) MC05 dataset. (**B**) MC06 dataset.

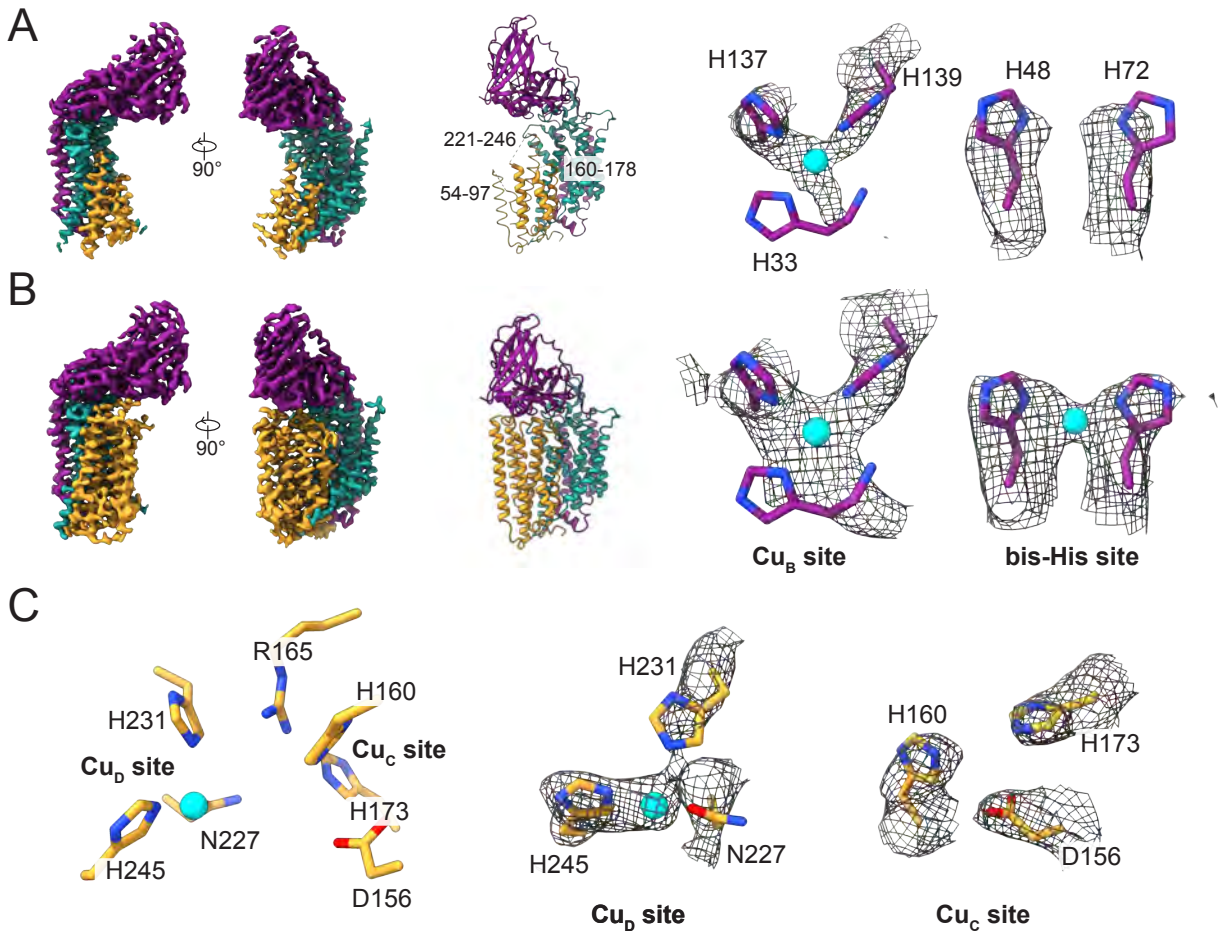

Fig. S21. Structure of potassium cyanide (KCN)-treated pMMO from *M. capsulatus* (Bath) reconstituted into nanodiscs. (**A**) A single protomer from the 3.65 Å resolution map of KCN-treated pMMO in a native lipid nanodisc with no added copper (MC05) and the model with missing residues labeled. The Cu_B and bis-His sites are shown at the same threshold level. (**B**) A single protomer from the 3.39 Å map of KCN-treated pMMO with copper added back before pMMO isolation and during reconstitution into native lipid nanodiscs (MC06). The complete model is shown along with the Cu_B and bis-His sites at the same threshold. (**C**) PmoC metal-binding sites in MC06. Cu_C and Cu_D are shown at the same threshold level. Residues in the Cu_D site are not as well defined, although there is a strong density near the location of the Cu_D metal ion in the other, high resolution maps (MC01, MC02, MC04). The Cu_C residues fit well into the density, although there is no evidence for metal occupancy.

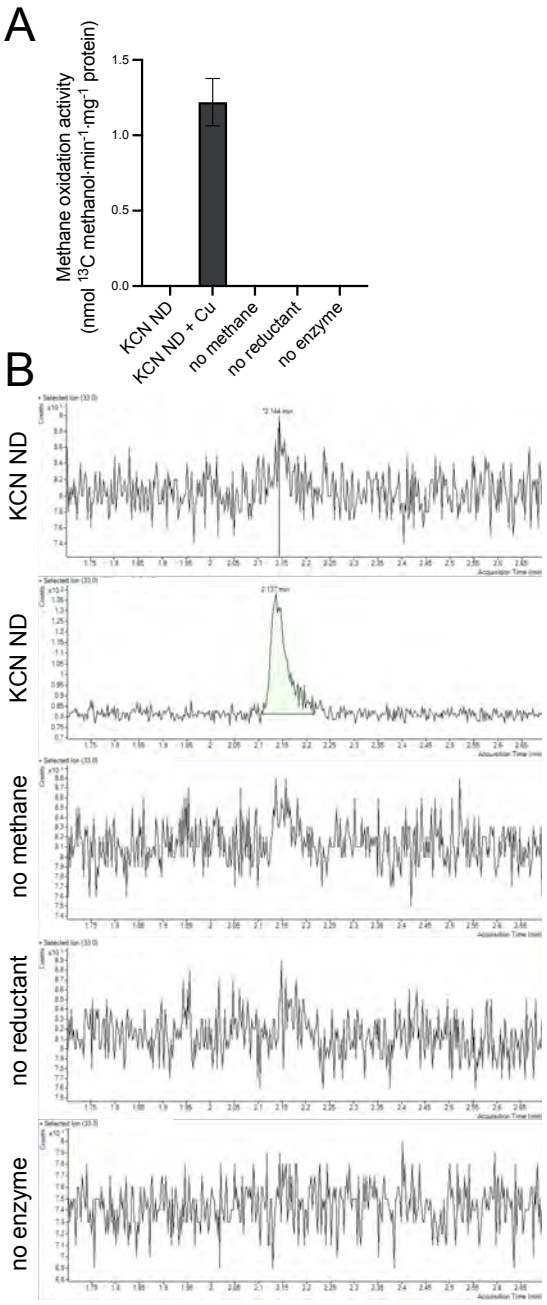

Fig S22. Methane oxidation by pMMO treated with potassium cyanide (KCN). (**A**) KCN ND, nanodiscs formed with pMMO from the KCN-treated membranes and native lipids; KCN ND + Cu, copper added back to KCN-treated membranes followed by pMMO isolation from those membranes and reconstitution into nanodiscs with native lipids. Error bars represent standard deviation of n = 2 biological replicates, each measured in triplicate. (**B**) GC/MS traces measuring +33 ion corresponding to ^{13}C-methanol for the native nanodisc sample.

Table S1. pMMO activity data

Sample	Methanotroph	Substrate	Reductant	Turnover number per protomer (s^{-1})	Specific activity (nmol mg total protein^{-1} min^{-1})	References
Cells producing pMMO	*M. capsulatus* (Bath)	propylene	formate	1.4-2.5[a]	167-300	(*56, 57*)
	M. trichosporium OB3b	methane	NA	0.68-2.5[b]	82-300	(*58, 59*)
Membrane-bound pMMO	*M. capsulatus* (Bath)	methane	NADH	0.083-0.146[c]	40-70	(*11*)
			duroquinol	0.026-0.042[d]	12-20	(*10*)
		propylene	NADH	0.044-0.246[e]	21-118	(*56, 60*)
			duroquinol	0.033-0.179[e]	16-86	(*56, 60*)
	M. sp. str. Rockwell	methane	NADH	0.017-0.024[d,f]	8-11.5	(*10*)
			duroquinol	0.004-0.006[d,f]	1.8-3	(*10, 14*)
	M. alcaliphilum 20Z	methane	NADH	0.006[c,f]	3	(*11*)
			duroquinol	0	0	(*11*)
Purified pMMO in DDM[g]	*M. capsulatus* (Bath)	methane	NADH	0	0	(*11*)
			duroquinol	0.002[h,i]	1	(*11*), this work
	M. capsulatus (Bath)	propylene	NADH	0	0	(*56, 60*)
			duroquinol	0.032-0.21[i,j]	18-126	(*56, 60*)
	M. sp. str. Rockwell	methane	NADH	0	0	(*10*)
			duroquinol	0	0	(*10*)
	M. alcaliphilum 20Z	methane	NADH	0	0	(*11*)
			duroquinol	0	0	(*11*)
Purified pMMO in bicelles	*M. capsulatus* (Bath)	methane	NADH	0.009[f,h]	5.2	(*11*)
			duroquinol	0.006[f,h]	3.5	(*11*)
	M. alcaliphilum 20Z	methane	NADH	0	0	(*11*)
			duroquinol	0.007[f,h]	4.4	(*11*)
Purified pMMO in nanodiscs[i]						
DMPC[g]	*M. capsulatus* (Bath)	methane	duroquinol	0.005[h]	3	this work
POPC[g]	*M. capsulatus* (Bath)			0.009[h]	5.4	this work
native lipids	*M. capsulatus* (Bath)			0.012[h]	7.2	this work
POPC[g]	*M.* sp. str. Rockwell	methane	duroquinol	0.011[h]	6.6	(*14*)
POPC[e]	*M. alcaliphilum* 20Z	methane	duroquinol	0	0	this work

[a]Calculated from rate of propylene epoxidation monitored by gas chromatography (GC) and assuming pMMO is 20% of the total protein

[b]Calculated from rate of methane uptake and assuming that pMMO is 20% of the total protein.

[c]Calculated from rate of conversion of $^{13}CH_4$ to $^{13}CH_3OH$ monitored by GC/mass spectrometry (GC/MS) and assuming that membrane-bound protein is 80% pMMO.

[d]Calculated from rate of conversion of CH_4 to CH_3OH monitored by GC and assuming that membrane-bound protein is 80% pMMO. Values from (*10*) were converted to ^{13}C values by applying a correction factor of 0.5 (*11*).

[e]Calculated from rate of propylene epoxidation monitored by GC and assuming that membrane-bound protein is 80% pMMO.

[f]Activity assay was performed at 30 °C. All other activity assays were performed at 45 °C.

[g]Abbreviations used: DDM, n-dodecyl-β-D-maltoside; DMPC, 1,2-dimyristoyl-sn-glycero-3-phosphocholine; POPC, 1-palmitoyl-2-oleoylphosphatidylcholine.

[h]Calculated from rate of conversion of $^{13}CH_4$ to $^{13}CH_3OH$ monitored by GC/MS.

[i]The samples used for the *M. capsulatus* (Bath) pMMO crystal structure determination were not assessed for methane oxidation activity and did not exhibit propylene epoxidation activity (*8*).

[j]Calculated from rate of propylene epoxidation monitored by GC.

Table S2. CryoEM data collection, refinement, and validation statistics

Sample	**MC01**	**MC02**	**MC03**	**MC04**	**20Z01**	**RW01**	**MC05**	**MC06**
Species	*M. capsulatus* (Bath)	*M. capsulatus* (Bath)	*M. capsulatus* (Bath)	*M. capsulatus* (Bath)	*M. alcaliphilum* 20Z	*M.* sp. str. Rockwell	*M. capsulatus* (Bath)	*M. capsulatus* (Bath)
Lipid type	native	POPC	native	native	POPC	POPC	native	native
PDB code	7S4H	7S4I	7S4J	7S4K	7S4L	7S4M	7T4O	7T4P
EMDB code	24827	24828	24829	24830	24831	24832	25683	25684
Data collection and processing								
Center	PNCC	PNCC	SLAC	NCCAT	NCCAT	SLAC	PNCC	PNCC
Microscope	Titan Krios-3							
Voltage (kV)	300							
Camera	Gatan K3							
Magnification	30k	30k	40k	30k	30k	30k	40k	30k
Magnification at detector (Å/pixel)	1.02	1.02	0.86	1.05	1.07	1.04	0.84	1.07
Total electron exposure ($e^-/Å^2$)	54	52	50	64	64	40	50	50
Defocus range (μm)	-2.0 to -4.0							
Automation software	SerialEM							
Energy filter slit width (eV)	n. a.	n. a.	20	20	20	20	n. a.	n. a.
Micrographs collected	9,081	10,889	9,966	11,593	6,564	3,565	4,601	9,405
Reconstruction								
Refined particles	1,381,649	1,477,719	881,128	546,332	443,800	490,196	394,208	812,752
Symmetry	C3							
Resolution, FSC 0.143 (Å)	2.14	2.26	2.16	2.36	2.46	2.42	3.65	3.39
Map sharpening B factor ($Å^2$)	-69	-70	-72	-69	-120	-101	-181	-154

Map sharpening methods	Coot							
Model composition								
Protein residues	2577	2577	2577	2577	2619	2574	2310	2574
Ligands	63	63	54	63	36	27	27	54
Waters	410	355	304	110	14	36	0	0
Model Refinement								
Refinement package	Phenix							
Real or reciprocal space	Real							
Model-Map scores								
CC	0.84	0.84	0.82	0.89	0.87	0.59	0.78	0.83
Average FSC B factors ($Å^2$)								
Protein Residues	43.93	41.92	49.84	68.38	74.03	141.00	85.92	21.51
Ligands	20.27	20.27	20.16	20.38	83.19	73.68	20.75	20.23
Waters	39.80	38.25	44.97	59.73	72.96	135.02	n. a.	n. a.
R.m.s. deviations								
Bond lengths (Å)	0.009	0.009	0.010	0.010	0.006	0.009	0.007	0.010
Bond Angles (°)	1.110	1.266	1.318	1.340	1.012	1.262	0.903	1.110
Validation								
MolProbity score	2.36	2.48	2.51	2.41	2.71	2.65	2.30	2.20
CaBLAM outliers	2.95	3.19	2.72	2.95	3.29	3.52	2.95	2.60
Clashscore	14.25	15.60	13.55	13.41	24.10	13.99	16.49	19.10
Rotamer outliers (%)	2.83	3.29	4.30	3.29	3.26	6.06	1.85	0.82
C-beta deviations (%)	0.13	0.00	0.04	0.13	0.00	0.08	0.00	0.13
Ramachandran plot								
Favored (%)	94.92	94.29	94.33	94.37	92.95	94.04	94.37	93.51
Outliers (%)	0.23	0.47	0.51	0.23	0.35	0.42	0.26	0.35